Journal of Luminescence 182 (2017) ∎∎∎–∎∎∎

Contents lists available at ScienceDirect

Journal of Luminescence

journal homepage: www.elsevier.com/locate/jlumin

Full Length Article

Excitation and emission spectra of $LaInO_3$-based solid solutions doped with Sm^{3+}, Sb^{3+}

E.K. Yukhno [a], L.A. Bashkirov [a,*], P.P. Pershukevich [b], I.N. Kandidatova [a], N. Mironova-Ulmane [c], A. Sarakovskis [c]

[a] Belarusian State Technological University, 13a Sverdlova Str., Minsk 220006, Belarus
[b] Stepanov's Institute of Physics, Belarusian National Academy of Sciences, 68 Nezavisimosti Ave., Minsk 220072, Belarus
[c] Institute of Solid State Physics, University of Latvia, 8 Kengaraga Str., Riga LV-1063, Latvia

ARTICLE INFO

Article history:
Received 23 November 2015
Received in revised form
18 July 2016
Accepted 11 October 2016

Keywords:
$LaInO_3$:Sm^{3+}
Sb^{3+}
Solid solution
Photoluminescence
Sensitizer

ABSTRACT

X-ray analysis showed that all the ceramic samples of $La_{1\text{-}x}Sm_xInO_3$ ($0.010 \le x \le 0.025$) solid solutions were single-phased but the samples of nominal composition of $LaIn_{0.98}Sb_{0.02}O_3$, $La_{0.98}Sm_{0.02}In_{0.98}Sb_{0.02}O_3$ contained a small amount of impurity phase of $LaSbO_3$-based solid solutions. It was established that $La_{0.98}Sm_{0.02}InO_3$ solid solution under the excitation of 275 nm and 320 nm exhibits the strongest photoluminescence among $La_{1\text{-}x}Sm_xInO_3$ solid solutions with $0.010 \le x \le 0.025$. Photoluminescence bands located in wavelength ranges of 550–580 nm, 585–625 nm and 630–680 nm exhibit 2–3 clear maxima each. According to the locations of these maxima we calculated the magnitudes of Stark splitting of $^6H_{5/2}$, $^6H_{7/2}$, $^6H_{9/2}$ multiplets of the main ^6H term of Sm^{3+} ion by crystal field of $La_{1\text{-}x}Sm_xInO_3$ solid solutions with orthorhombically distorted perovskite structure. It was established that the intensity of PL spectra obtained at $\lambda_{ex}=320$, 405 and 470 nm is significantly higher for sample of $La_{0.98}Sm_{0.02}In_{0.98}Sb_{0.02}O_3$ nominal composition than that of $La_{0.98}Sm_{0.02}InO_3$ solid solution. It could be explained by sensitizing effect of Sb^{3+} ions on Sm^{3+} ions photoluminescence or by higher PL intensity of Sm^{3+} ions of impurity phase than of $LaInO_3$ matrix.

1. Introduction

In the past ten years much attention was drawn to optical properties of perovskite $LaInO_3$-based solid solutions doped with RE ions (RE=Pr^{3+}, Sm^{3+}, Eu^{3+}, Tb^{3+}) and/or Bi^{3+} ion because of their visible light emission [1–4]. Substitution of La^{3+} ions by Bi^{3+} ions in $LaInO_3$: Eu^{3+} shows sensitizing effect on Eu^{3+} luminescence [3]. Sb^{3+} ions have $5s^2$ electron configuration similar to $6s^2$ electron configuration of Bi^{3+} ions. So Sb^{3+} ions are expected to be efficient sensitizer of RE ions. Luminescent properties of Sb^{3+} and Bi^{3+} ions in $LnBO_3$ (Ln=Sc, Y, La, Gd, Lu) were investigated in [5–10]. In these compounds Sb^{3+} and Bi^{3+} ions are located in Ln^{3+} ions sublattice. Bi^{3+} ions are sensitizers of Eu^{3+} luminescence in (Y, Gd)BO_3 and energy transfer is $Bi^{3+} \rightarrow Gd^{3+} \ldots Gd^{3+} \rightarrow Eu^{3+}$ [6,7]. At the same time in the work [8] no energy transfer between Sb^{3+} ions and Eu^{3+} ions in YBO_3-based solid solution was observed and both Sb^{3+} and Eu^{3+} ions acted as co-activators. There is no research devoted to luminescent properties of Sb^{3+} ions located in In^{3+} ions sublattice of $LaInO_3$. Such a substitution is possible because Sb^{3+} ionic radius is only 0.02 Å less than that of In^{3+} ($r_{In^{3+}}=0.92$ Å [11]) and 0.14 Å less than that of La^{3+} ($r_{La^{3+}}=1.04$ Å [11]). In the present work we investigate excitation and emission spectra of $LaIn_{0.98}Sb_{0.02}O_3$, $La_{0.98}Sm_{0.02}In_{0.98}Sb_{0.02}O_3$ and $La_{1\text{-}x}Sm_xInO_3$ ($0.010 \le x \le 0.025$) solid solutions. All $LaInO_3$-based solid solutions were synthesized by solid-state reaction method and had the structure of orthorhombically distorted perovskite.

2. Experimental

$LaInO_3$ indate and $La_{1\text{-}x}Sm_xInO_3$ (x=0.010, 0.015, 0.020, 0.025), $LaIn_{0.98}Sb_{0.02}O_3$, $La_{0.98}Sm_{0.02}In_{0.98}Sb_{0.02}O_3$ solid solutions ceramic samples were synthesized by solid-state reaction method using mixture of La_2O_3 (99.99%), Sm_2O_3 (99.99%), In_2O_3 (99.99%) and Sb_2O_3 (99.99%) oxides. La_2O_3 and Sm_2O_3 were preheated at 1273 K for 1 h. Stoichiometric amounts of the reactants were mixed with the aid of ethanol, ground in planetary mill (Pulverizette Fritch) in cups with zirconia balls and then pressed in pellets (D=25 mm, h=5–7 mm). The pellets were sintered at 1523 K for 6 h on the Al_2O_3 substrate. The pellets of different composition were not in contact with each other. In order to prevent the pellet-substrate

---

[*] Corresponding author.
E-mail address: bashkirov@belstu.by (L.A. Bashkirov).

http://dx.doi.org/10.1016/j.jlumin.2016.10.020
0022-2313/

interaction the pellets were separated from the substrate by thin powder layer of the same composition. Then the pellets were ground, milled and pressed in bars (5 × 5 × 30 mm). The bars were finally sintered at 1523 K for 6 h. The compounds were characterized by powder X-ray diffraction (XRD) analysis (Bruker D8 Advance) at room temperature using CuKα radiation. Crystal structure parameters of the investigated compounds have been calculated using X-ray structure tabular processor (RTP). SEM-images of indates were obtained with scanning electronic microscope JEOL JSM-5610LV with assistance of Energy Dispersive X-ray Spectrometer JED 22-01. Excitation and emission spectra of ceramic samples were recorded at 300 K using automatic spectrofluorometer SDL-2 composed of MDR-12 high-aperture excitation monochromator and MDR-23 recording monochromator at the Institute of Physics of the National Academy of Sciences of Belarus. Xe-lamp DKsSh-120 was used as excitation source.

3. Results and discussion

XRD patterns of $LaInO_3$ indate and $La_{1-x}Sm_xInO_3$ (x=0.010, 0.015, 0.020, 0.025) solid solutions (Fig. 1a) showed that all the samples were single-phased and had the structure of orthorhombically distorted perovskite ($GdFeO_3$-type, $a < c/\sqrt{2} < b$ [12]). Crystal structure parameters a, b, c and crystal cell volume V are presented in Table 1. Samples with nominal composition of $LaIn_{0.98}Sb_{0.02}O_3$ and $La_{0.98}Sm_{0.02}In_{0.98}Sb_{0.02}O_3$ had on their XRD patterns (Fig. 1a) not only the peaks corresponding to main perovskite phase but also one impurity peak of small intensity (d=3.104 Å, 2Θ=28.76° for $La_{0.98}Sm_{0.02}In_{0.98}Sb_{0.02}O_3$ sample; d=3.111 Å, 2Θ=28.70° for $LaIn_{0.98}Sb_{0.02}O_3$ sample). This reflex is probably referred to not-reacted Sb_2O_3 oxide or to intermediate $LaSbO_3$ compound which is formed during synthesis. The most intensive reflexes d parameters for that samples are [13,14] 3.151 and 3.196 Å, respectively. In order to identify the origin of the impurity phase in agate mortar there was made a mixture of $La_{0.98}Sm_{0.02}InO_3$ and Sb_2O_3 compounds with Sm^{3+}: Sb^{3+} ions ratio 1:1. On the XRD pattern of the mixture no peak of Sb_2O_3 phase was observed. The $LaIn_{0.98}Sb_{0.02}O_3$ sample was additionally sintered at 1523 K for 6 h. The impurity reflex intensity on the XRD pattern of additionally sintered sample did not decreased and remained the same (Fig. 1a). So the impurity reflex is probably referred to $LaSbO_3$ and $La_{1-y}Sm_ySbO_3$ solid solutions on its base. The ratio if intensities of the highest reflexes of the impurity phase (2Θ=28.70°) and the main phase (2Θ=30.65°) shows that in the $LaIn_{0.98}Sb_{0.02}O_3$ sample the amount of impurity phase is about 5% of the main phase. On SEM-images of $La_{0.98}Sm_{0.02}InO_3$, $La_{0.98}Sm_{0.02}In_{0.98}Sb_{0.02}O_3$, $LaIn_{0.98}Sb_{0.02}O_3$ ceramic samples (Fig. 1b) no sign of other phase was observed. Grain size was estimated to be about 0.5–3 µm.

Table 1
Cell parameters (a, b, c), cell volume (V) and orthorhombical distortion degree (ε) for $LaInO_3$ and $LaInO_3$-based solid solutions doped with Sm^{3+}, Sb^{3+}.

Composition	Cell parameters					$c/\sqrt{2}$,Å
	a, Å	b, Å	c, Å	V, Å^3	$\varepsilon \cdot 10^2$	
$LaInO_3$	5.738	5.953	8.227	281.0	3.75	5.817
$La_{0.99}Sm_{0.01}InO_3$	5.732	5.943	8.228	280.3	3.68	5.818
$La_{0.985}Sm_{0.015}InO_3$	5.731	5.944	8.228	280.3	3.72	5.818
$La_{0.98}Sm_{0.02}InO_3$	5.732	5.944	8.223	280.2	3.70	5.814
$La_{0.975}Sm_{0.025}InO_3$	5.724	5.939	8.224	279.5	3.76	5.815
$La_{0.98}Sm_{0.02}In_{0.98}Sb_{0.02}O_3$	5.731	5.932	8.229	279.8	3.51	5.819
$LaIn_{0.98}Sb_{0.02}O_3$	5.735	5.937	8.234	280.3	3.52	5.822

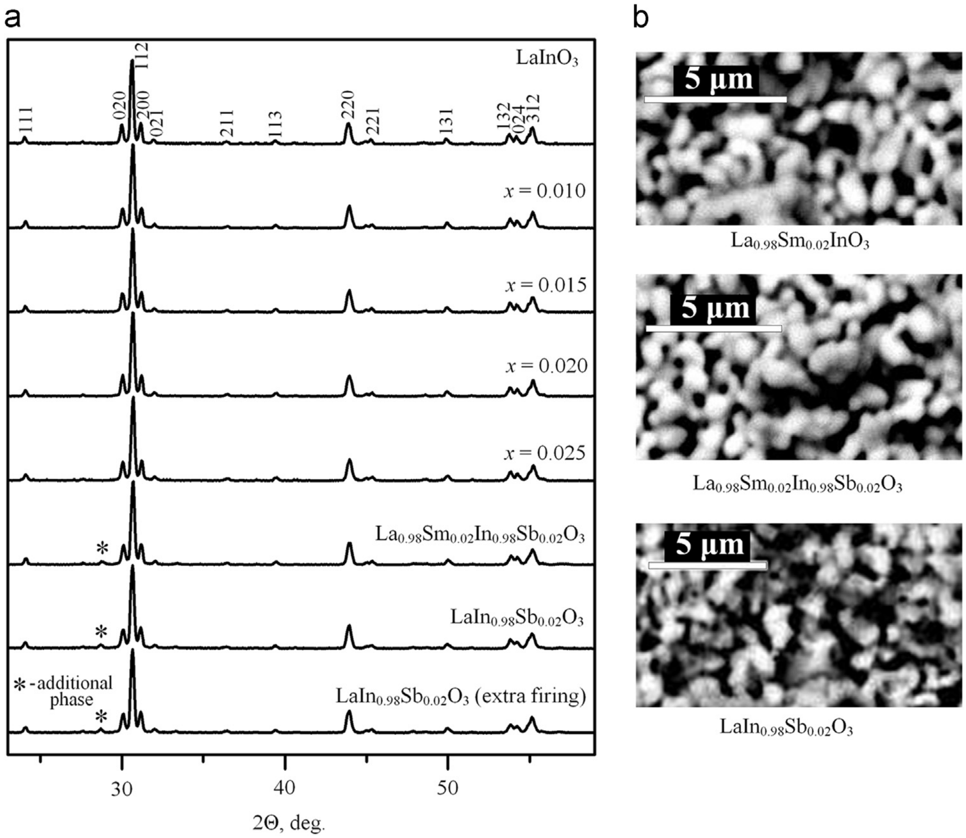

$La_{0.98}Sm_{0.02}InO_3$

$La_{0.98}Sm_{0.02}In_{0.98}Sb_{0.02}O_3$

$LaIn_{0.98}Sb_{0.02}O_3$

Fig. 1. XRD patterns of $LaInO_3$, $La_{1-x}Sm_xInO_3$ (x=0.01, 0.015, 0.02, 0.025), $La_{0.98}Sm_{0.02}In_{0.98}Sb_{0.02}O_3$, $LaIn_{0.98}Sb_{0.02}O_3$ (a); SEM-images of $La_{0.98}Sm_{0.02}InO_3$, $La_{0.98}Sm_{0.02}In_{0.98}Sb_{0.02}O_3$ and $LaIn_{0.98}Sb_{0.02}O_3$ ceramic samples (b).

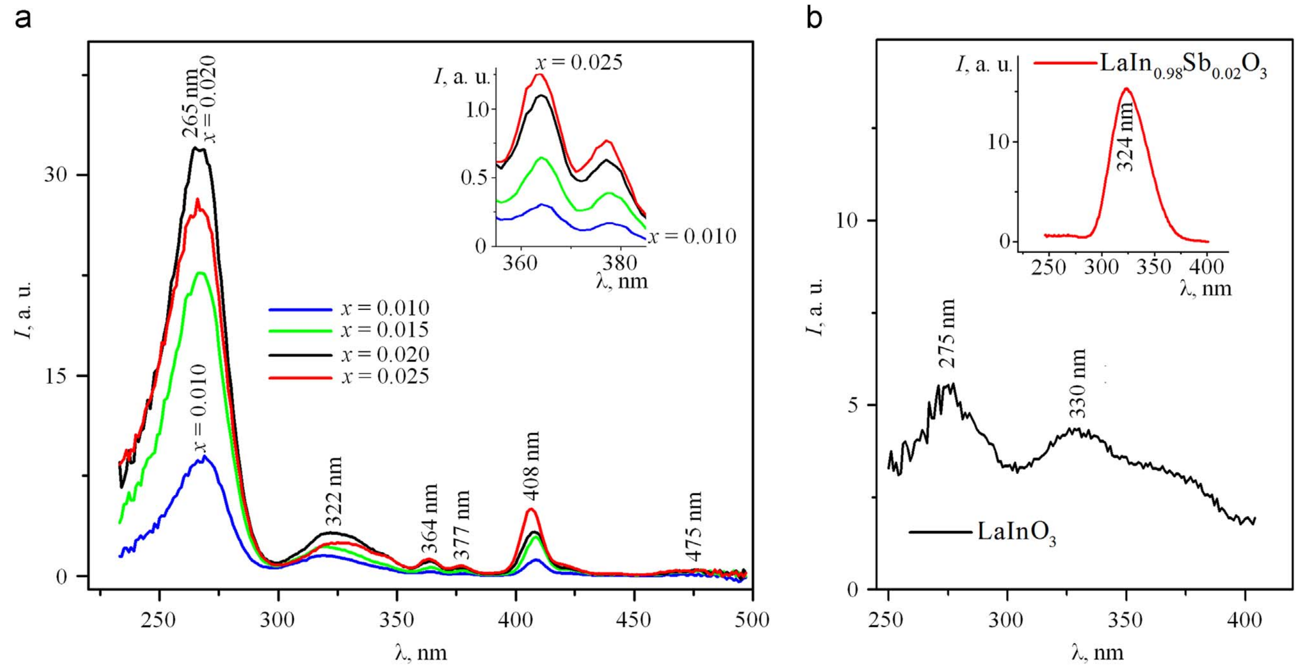

Fig. 2. Excitation ($\lambda_{mon}=602$ nm) spectra of $La_{1-x}Sm_xInO_3$ ($x=0.01$, 0.015, 0.02, 0.025) solid solutions (a); excitation spectra of $LaInO_3$ ($\lambda_{mon}=433$ nm) and $LaIn_{0.98}Sb_{0.02}O_3$ ($\lambda_{mon}=450$ nm, inset) (b).

Since $LaInO_3$ and its solid solutions formation mechanism has not been investigated let us pay attention to some conditions of its synthesis by solid state reactions method induced by reciprocal or irreciprocal electrons or cations and oxygen ions diffusion. Solid state reactions proceed on reactants contacting particles interface. In present work solid state synthesis of $LaInO_3$-based solid solutions (e.g. $La_{0.98}Sm_{0.02}In_{0.98}Sb_{0.02}O_3$) was performed by sintering on air at 1523 K of La_2O_3, In_2O_3, Sm_2O_3, Sb_2O_3 oxides mixture of certain molar ratios. After milling the mixture contains various pairs of contacting particles referred to identical or different oxides. Let us suppose that a certain volume contains of reactants particles equal number of moles of certain oxide. The number of pairs of contacting particles of identical or different oxides depends on number of each oxide particles. In starting mixture for $La_{0.98}Sm_{0.02}In_{0.98}Sb_{0.02}O_3$ solid solution synthesis the number of La_2O_3, In_2O_3 particles is approximately 49 times higher (0.98/0.02) than Sm_2O_3, Sb_2O_3 particles. Therefore, in such a mixture the number of La_2O_3–In_2O_3 contacting pairs is many times higher than that of La_2O_3–Sm_2O_3, La_2O_3–Sb_2O_3 contacting pairs. The number of Sm_2O_3–Sb_2O_3 contacting pairs is many times lower than that of La_2O_3–Sm_2O_3, La_2O_3–Sb_2O_3, In_2O_3–Sm_2O_3 and In_2O_3–Sb_2O_3 contacting pairs. Due to that during sintering of La_2O_3, In_2O_3, Sm_2O_3, Sb_2O_3 oxides mixture designed for $La_{0.98}Sm_{0.02}In_{0.98}Sb_{0.02}O_3$ solid solution synthesis the probability of intermediate $SmSbO_3$ compound and $La_{1-y}Sm_ySbO_3$ solid solution formation is much lower than that of $LaInO_3$ compound, $LaInO_3$-based solid solutions, $SmInO_3$ compound and $In_{2-y}Sb_yO_3$ solid solution. Hence, despite of a small amount ($\approx 5\%$) of impurity phase of $LaSbO_3$ or

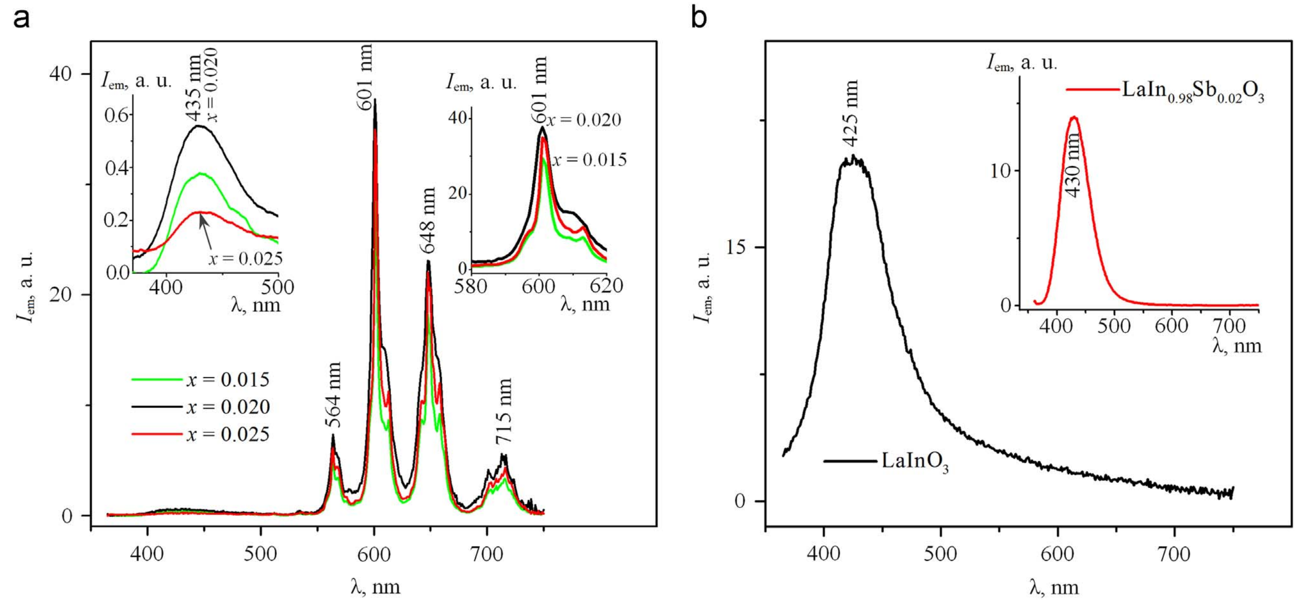

Fig. 3. Emission ($\lambda_{ex}=275$ nm) spectra of $La_{1-x}Sm_xInO_3$ ($x=0.015$, 0.02, 0.025) solid solutions (a); emission spectra of $LaInO_3$ ($\lambda_{ex}=330$ nm) and $LaIn_{0.98}Sb_{0.02}O_3$ ($\lambda_{ex}=320$ nm, inset) (b).

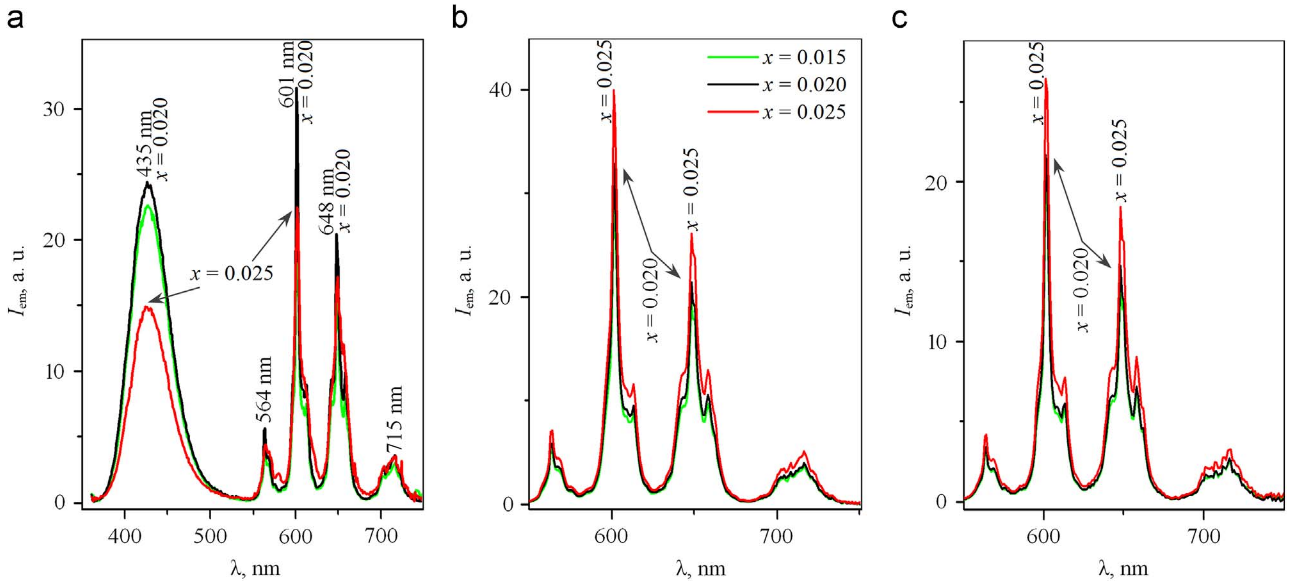

Fig. 4. Emission spectra of $La_{1-x}Sm_xInO_3$ ($x=0.015$, 0.02, 0.025) solid solutions with $\lambda_{ex}=320$ nm (a), 405 nm (b), 470 nm (c).

$La_{1-y}Sm_ySbO_3$ in a sample of $La_{0.98}Sm_{0.02}In_{0.98}Sb_{0.02}O_3$ nominal composition, only insignificant part of Sm^{3+}, Sb^{3+} ions transfers to impurity phase. Therefore, impurity phase existence in Sb^{3+} containing samples only insignificantly decreases set Sm^{3+}, Sb^{3+} ions concentration in $LaInO_3$-based solid solutions. This conclusion is confirmed by Table 1 data showing that crystal structure parameters *a*, *b* and crystal cell volume *V* of solid solutions of nominal composition of $La_{0.98}Sm_{0.02}In_{0.98}Sb_{0.02}O_3$ and $LaIn_{0.98}Sb_{0.02}O_3$ are insignificantly less than those of undoped $LaInO_3$, as Sm^{3+}, Sb^{3+} ionic radii are insignificantly less than La^{3+}, In^{3+} ionic radii. That proves that during $LaIn_{0.98}Sb_{0.02}O_3$, $La_{0.98}Sm_{0.02}In_{0.98}Sb_{0.02}O_3$ synthesis Sm^{3+} and Sb^{3+} ions were placed into crystal structure of $LaInO_3$ matrix so the main share of Sm^{3+} and Sb^{3+} ions is located in main phase and not in impurity phase.

Looking at Fig. 2a it is possible to conclude that the excitation bands intensity in excitation spectra of $La_{1-x}Sm_xInO_3$ ($x=0.010$, 0.015, 0.020, 0.025) solid solutions with $\lambda_{mon}=602$ nm depends on Sm^{3+} ions concentration. The strongest excitation band has a maximum at 265 nm ($\nu=37736$ cm^{-1}) and belongs to near UV region. For the excitation bands with maxima at 265 nm and 322 nm the highest intensity is observed for $La_{1-x}Sm_xInO_3$ solid solution with $x=0.020$ (Fig. 2a). For these bands of $La_{0.98}Sm_{0.02}InO_3$ sample their full-widths at the half maximum (FWHM) were 29 nm and 37 nm, respectively. For the excitation bands with maxima at 364 nm, 377 nm, 408 nm and the highest intensity is observed for $La_{1-x}Sm_xInO_3$ solid solution with $x=0.025$ (Fig. 2a, inset). According to [1] strong excitation band with maximum at 265 nm is caused by the oxygen (2*p*) to samarium (4*f*) charge transfer transition (O^{2-}–Sm^{3+}). In present work excitation spectra of undoped $LaInO_3$ with $\lambda_{mon}=433$ nm was obtained (Fig. 2b). On that spectrum there is a band with maximum at $\lambda_{max}=275$ nm that differs slightly from the maximum of $\lambda_{max}=265$ nm on excitation spectra of $La_{1-x}Sm_xInO_3$ (Fig. 2a). This band absents on excitation spectrum of $LaInO_3$ obtained in [2] and could be explained by Sm^{3+} ions contamination but the results of X-ray fluorescent analysis with high-energy X-rays excitation show that undoped $LaInO_3$ contains no Sm^{3+} ions. According to [1] excitation bands with maxima at 364 nm, 377 nm, 408 nm are due to 4*f*-electrons of Sm^{3+} ion transitions from the ground $^6H_{5/2}$ level to the excited levels $^4D_{15/2}$, $^4L_{17/2}$ and $^4K_{11/2}$, respectively [1]. In the excitation spectra of $La_{1-x}Sm_xInO_3$ ($x=0.010$, 0.015, 0.020, 0.025) solid solutions there is a well-defined band with a maximum at 322 nm (Fig. 2a). This band intensity depends on Sm^{3+} ions content in $La_{1-x}Sm_xInO_3$. Similar weak band was shown in the excitation spectrum of $La_{0.98}Sm_{0.02}InO_3$ solid solution presented in [1] its nature is not understood. On excitation band of undoped $LaInO_3$ (Fig. 2b) obtained in present work there is a wide asymmetrical band with blurred maximum at 330 nm (Fig. 2b). Similar symmetrical excitation band with maximum at 328 nm and FWHM of ≈ 40 nm was observed in [2] for $LaInO_3$ but was not observed for $LaAlO_3$: Sm^{3+} [15]. Hence, the origin of this band is electronic transition in $LaInO_3$ involving In^{3+} ions.

Photoluminescence (PL) spectra of $La_{1-x}Sm_xInO_3$ ($x=0.015$, 0.020, 0.025) solid solutions under the excitation at 275 nm

Table 2
Emission bands maxima wavelengths (λ_{em}) and energies (ν_{em}), Stark splitting magnitudes for $La_{1-x}Sm_xInO_3$ with $x=0.02$, 0.025, $La_{0.98}Sm_{0.02}In_{0.98}Sb_{0.02}O_3$ solid solutions after excitation of $\lambda_{ex}=275$ nm.

$La_{0.98}Sm_{0.02}InO_3$			$La_{0.975}Sm_{0.025}InO_3$			$La_{0.98}Sm_{0.02}In_{0.98}Sb_{0.02}O_3$	
λ_{em}, nm	ν_{em}, cm^{-1}	$\Delta\nu_{st}$, cm^{-1}	λ_{em}, nm	ν_{em}, cm^{-1}	$\Delta\nu_{st.}$, cm^{-1}	λ_{em}, nm	ν_{em}, cm^{-1}
435	22989	–	430	23256	–	434	23042
564	17730	93	564	17730	124	564	17730
567	17637		568	17606		567	17637
601	16639	192	601	16639	326	601	16639
608	16447		613	16313		613	16313
642	15576	144	643	15552	120	643	15552
648	15432	211	648	15432	234	648	15432
657	15221		658	15198		658	15198
715	13986	–	715	13986	–	716	13966

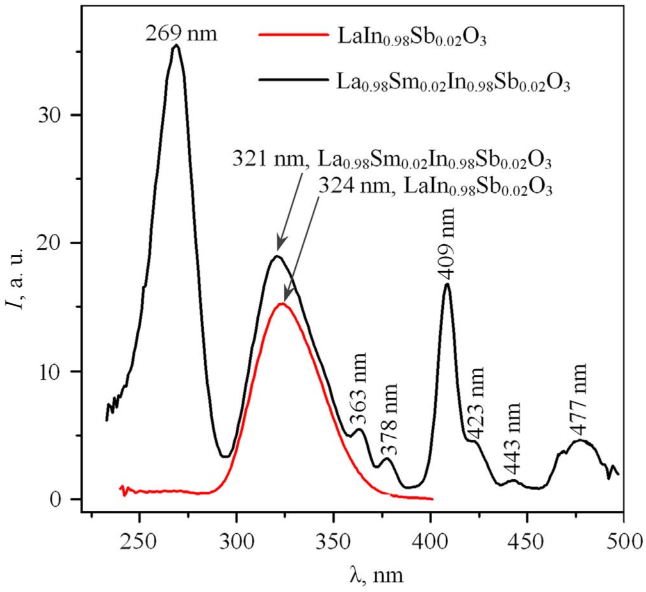

Fig. 5. Excitation spectra of $LaIn_{0.98}Sb_{0.02}O_3$ ($\lambda_{mon}=450$ nm) and $La_{0.98}Sm_{0.02}In_{0.98}Sb_{0.02}O_3$ ($\lambda_{mon}=602$ nm) solid solutions.

(Fig. 3a), 320 nm, 405 nm, 470 nm (Fig. 4) were measured. In the visible green-red region (550–750 nm) these spectra consist of four bands. For those bands their maxima in $La_{1-x}Sm_xInO_3$ ($x=0.020$, 0.025) solid solutions under the excitation at 275 nm are presented in Table 2. Additional luminescence band located between 400 and 500 nm is present in the PL spectra of $La_{1\text{-}x}Sm_xInO_3$ solid solutions (Fig. 3a, inset, Fig. 4 a). This band intensity depends on excitation wavelength and Sm^{3+} ions content. On PL spectrum of undoped $LaInO_3$ (Fig. 3b) there is a band with maximum at 425 nm. Similar symmetrical band with maximum at 426 nm and FWHM of ≈ 53 nm was observed in [2]. On PL spectra ($\lambda_{ex}=252$ nm) of $LaGaO_3$ solid solution doped with 1% of Sm^{3+} ions there was observed a band with maximum of 435 nm caused by charge transfer from 2*p*-sublevel of oxygen ions to free 4*s* sublevel of Ga^{3+} ions [16]. In^{3+} ions have $5d^{10}$ electron configuration similar to $4d^{10}$ electron configuration of Ga^{3+} ions. So we can suppose that PL band of $La_{0.98}Sm_{0.02}InO_3$ solid solution with maximum at 435 nm is also due to charge transfer from 2*p*-sublevel of oxygen ions to free 5*s* sublevel of In^{3+} ions. Other PL bands intensity of $La_{1-x}Sm_xInO_3$ ($0.015 \le x \le 0.025$) solid solutions investigated depends on Sm^{3+} doping concentration. Under the excitation of 275 nm and 320 nm maximum PL intensity was observed for $La_{1-x}Sm_xInO_3$ solid solution with $x=0.020$ (Fig. 3a, inset, Fig. 4a). Under the excitation at 405 nm and 470 nm maximum PL intensity was observed for $La_{1-x}Sm_xInO_3$ solid solution with $x=0.025$ (Fig. 4b and c). This correlates well with the PL spectrum data obtained under the excitation of 268 nm which is presented in work [1].

According to [1,17] PL bands with maxima at 564 nm, 601 nm, 648 nm and 715 nm (Table 2) are caused by 4*f*-electrons of Sm^{3+} ion transitions from the excited $^4G_{5/2}$ level to the levels with lower energy $^6H_{5/2}$, $^6H_{7/2}$, $^6H_{9/2}$, and $^6H_{11/2}$, respectively. PL bands located in wavelength ranges of 550–580 nm and 585–625 nm have 2 clear maxima each while PL band between 630 and 680 nm has 3 clear maxima (Figs. 3a and 4). Such splitting of the PL bands into 2–3 close maxima could be caused by Stark splitting of $^6H_{5/2}$, $^6H_{7/2}$, $^6H_{9/2}$ multiplets of ^6H term of Sm^{3+} ion by crystal field of $La_{1\text{-}x}Sm_xInO_3$ solid solutions orthorhombically distorted perovskite structure. The clearest triplet splitting is observed for $La_{1\text{-}x}Sm_xInO_3$ solid solution with $x=0.025$ which PL intensity is close to that of $La_{1\text{-}x}Sm_xInO_3$ solid solution with $x=0.020$. In Table 2 Stark splitting of ^6H term magnitudes are calculated by closely located pairs of PL maxima for $La_{1\text{-}x}Sm_xInO_3$ solid solution with $x=0.020$, 0.025.

Energy intervals between two multiplets $^6H_{5/2}$–$^6H_{7/2}$, $^6H_{7/2}$–$^6H_{9/2}$, $^6H_{9/2}$–$^6H_{11/2}$ ($\Delta\nu_{mult}$) were calculated as the difference between wavenumbers of the first PL maximum in the short wave region. These energy intervals for $La_{0.98}Sm_{0.02}InO_3$ solid solution were calculated using its PL spectra under the excitation at 275 nm and they are equal to 1091 cm^{-1}, 1063 cm^{-1} and 1590 cm^{-1}, respectively. The calculated value of $^6H_{5/2}$–$^6H_{7/2}$ energy interval agree well with the literature data [18]. The values of the energy intervals calculated for other $La_{1\text{-}x}Sm_xInO_3$ solid solutions under different excitation are not significantly different. On Fig. 5 there are presented excitation spectrum ($\lambda_{mon}=450$ nm) of solid solution of nominal composition of $LaIn_{0.98}Sb_{0.02}O_3$ and excitation spectrum ($\lambda_{mon}=602$ nm) of solid solution with approximate

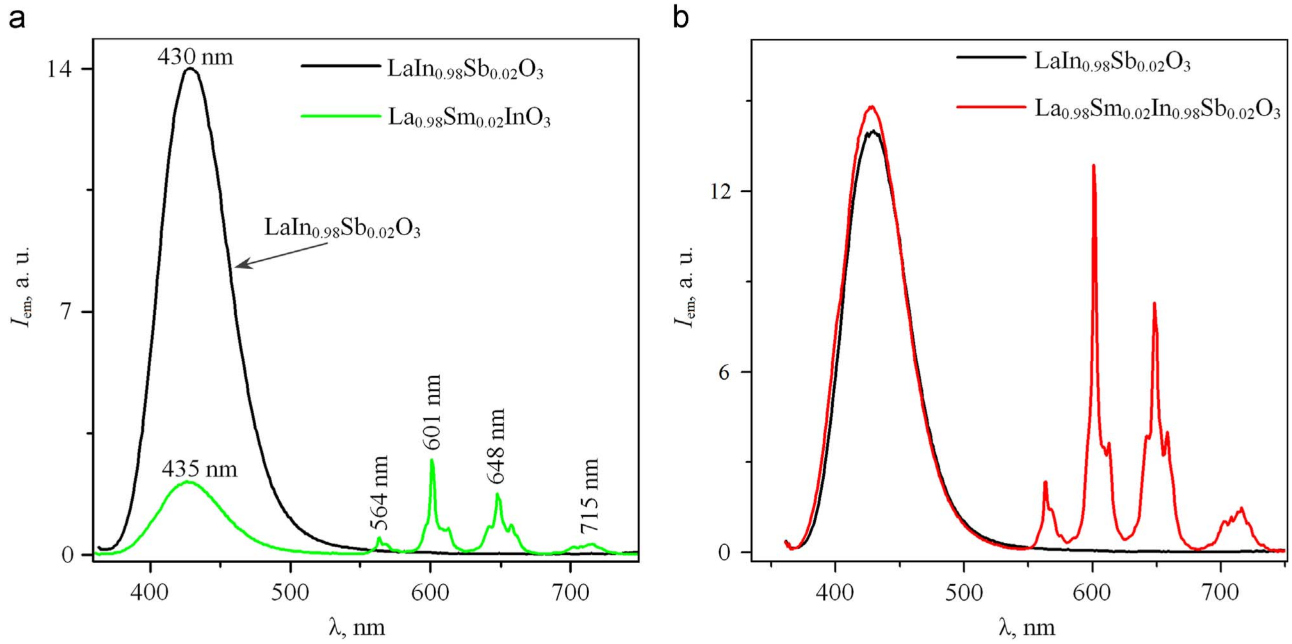

Fig. 6. Emission spectra ($\lambda_{ex}=320$ nm) of $LaIn_{0.98}Sb_{0.02}O_3$, $La_{0.98}Sm_{0.02}InO_3$ solid solutions (a) and $LaIn_{0.98}Sb_{0.02}O_3$, $La_{0.98}Sm_{0.02}In_{0.98}Sb_{0.02}O_3$ (b) solid solutions.

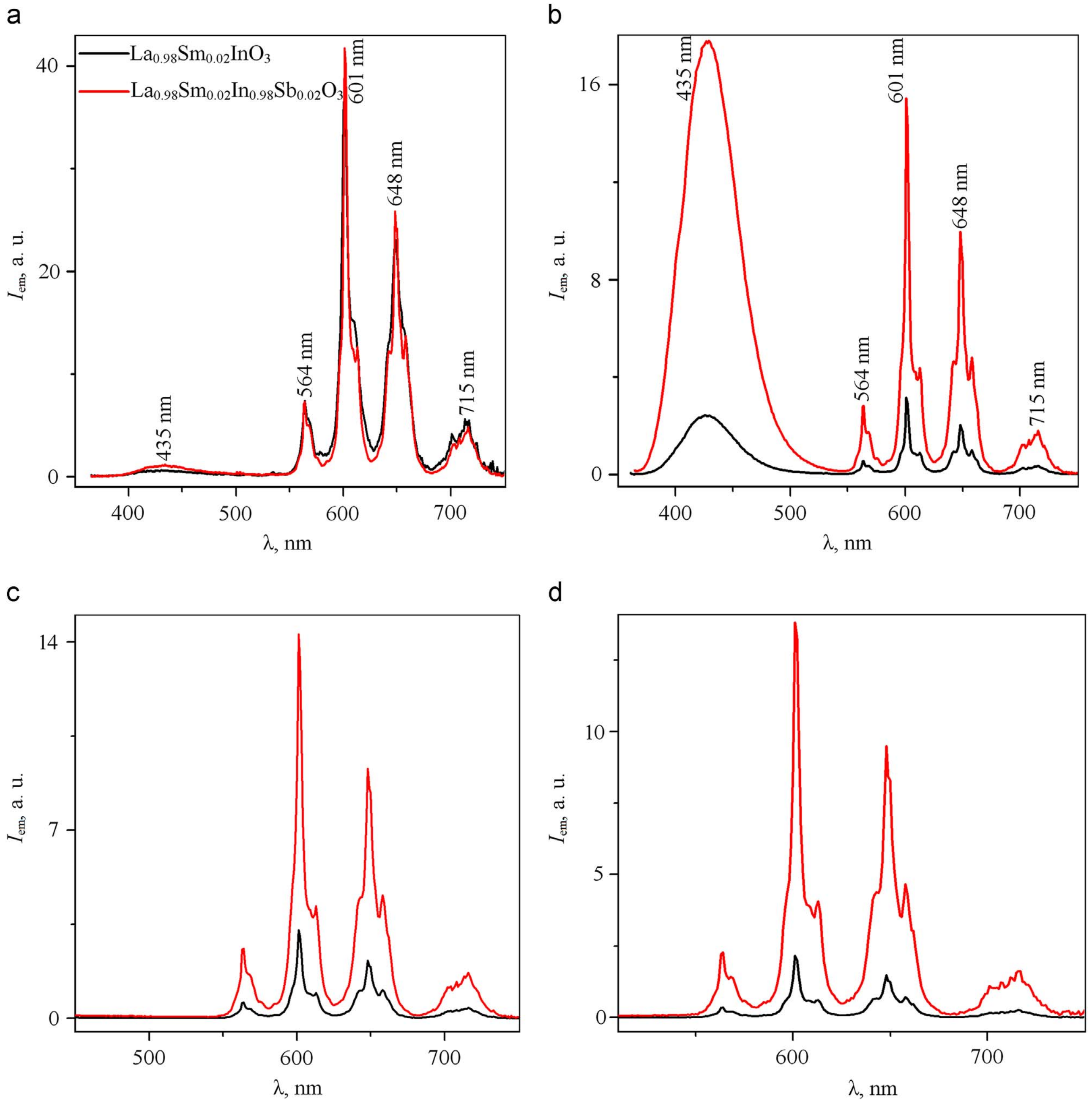

Fig. 7. Emission spectra of $La_{0.98}Sm_{0.02}InO_3$ and $La_{0.98}Sm_{0.02}In_{0.98}Sb_{0.02}O_3$ solid solutions with λ_{ex}=275 nm (a), 320 nm (b), 405 nm (c), 470 nm (d).

composition is $La_{0.98}Sm_{0.02}In_{0.98}Sb_{0.02}O_3$. As only insignificant part of Sm^{3+} and Sb^{3+} ions are in impurity phase this solid solution can be identified as $La_{0.98}Sm_{0.02}In_{0.98}Sb_{0.02}O_3$. Excitation spectrum of solid solution of nominal composition $LaIn_{0.98}Sb_{0.02}O_3$ (Fig. 2b inset, Fig. 5) consists of only one band of high intensity with maximum at 324 nm. That band overlaps with the excitation band of solid solution of nominal composition of $La_{0.98}Sm_{0.02}In_{0.98}Sb_{0.02}O_3$ with maximum at 321 nm (Fig. 5) and excitation band of undoped $LaInO_3$ with maximum at 330 nm (Fig. 2b). The excitation band of highest intensity in the excitation spectrum of $La_{0.98}Sm_{0.02}InO_3$ solid solution has maximum at 265 nm (Fig. 2a) though there is no similar band in excitation spectrum of $LaIn_{0.98}Sb_{0.02}O_3$ (Fig. 5). In the excitation spectrum of $LaIn_{0.98}Sb_{0.02}O_3$ the band between 290 and 370 nm is almost symmetrical so there is only one excitation band in this wavelength interval. PL spectrum (λ_{ex}=320 nm) of $LaIn_{0.98}Sb_{0.02}O_3$ (Fig. 6a and b) between 350 nm and 750 nm consists of only one almost symmetrical band with maximum at 430 nm (ν=23256 cm^{-1}). Stokes shift for this PL band was calculated using the excitation maximum (30864 cm^{-1}) and emission maximum (23256 cm^{-1}) and is equal to 7608 cm^{-1}. This magnitude slightly differs from the literature magnitude of the Stokes shift for Sb^{3+} ions in $ScBO_3$ (7900 cm^{-1}) [5]. Calculated in this work excitation and PL bands maxima and Stokes shift for solid solution of nominal composition of $LaIn_{0.98}Sb_{0.02}O_3$ (324 nm, 430 nm, 7608 cm^{-1}, respectively) differ slightly from those of In^{3+} photoluminescence in $LaInO_3$ (328 nm, 426 nm, 7013 cm^{-1}, respectively) obtained in [2] and present work (330 nm, 425 nm, 6774 cm^{-1}, respectively). According to [19] energy transfer from sensitizer ions to activator ions is allowed in the case of the overlap of sensitizer PL band and activator absorption (excitation) band. $LaInO_3$ co-doped with Sb^{3+} and Sm^{3+} ions meets this condition. After excitation of 320 nm $LaIn_{0.98}Sb_{0.02}O_3$ solid solution exhibits Sb^{3+} emission with maximum at 430 nm (Fig. 6a) while $La_{0.98}Sm_{0.02}InO_3$ has excitation band with peak at 408 nm is referred to Sm^{3+} ion (Fig. 2a). Fig. 7 show PL spectra of $La_{0.98}Sm_{0.02}InO_3$ solid solution doped with only Sm^{3+} ions and solid solution of nominal composition of $La_{0.98}Sm_{0.02}In_{0.98}Sb_{0.02}O_3$ co-doped with Sb^{3+} and Sm^{3+} ions after excitation of 275, 320 nm, 405 nm and 470 nm. From spectra presented at Fig. 7 ($\lambda_{ex}=320$, 405, 470 nm) it is obvious that PL intensity of $La_{0.98}Sm_{0.02}In_{0.98}Sb_{0.02}O_3$ sample containing both Sm^{3+} and Sb^{3+} ions is significantly higher than that of $La_{0.98}Sm_{0.02}InO_3$ sample containing no Sb^{3+} ions. It can be explained by sensitizing effect of Sb^{3+} ions on Sm^{3+} photoluminescence solid solution. Although we can't exclude that the reason could be higher PL of Sm^{3+} and Sb^{3+} ions in $La_{1-y}Sm_ySbO_3$ matrix than in $LaInO_3$-based matrix. In accordance to that it is possible that PL intensity of samples containing both Sm^{3+} and Sb^{3+} ions is mainly due to impurity phase PL, but not that of main phase. For final answer to that question further research is needed.

4. Conclusion

The results show that $La_{0.98}Sm_{0.02}InO_3$ exhibits the strongest emission among $La_{1-x}Sm_xInO_3$ ($x=0.010$, 0.015, 0.020, 0.025) solid solution after the excitation at 275 nm and 320 nm. For excitation in visible region (405 nm and 470 nm) the highest PL intensity was observed for $La_{0.975}Sm_{0.025}InO_3$. PL bands located in the wavelength ranges in 550–580 nm, 585–625 nm and 630–680 nm split by crystalline field into 2–3 clear maxima. The magnitudes of Stark splitting of $^6H_{5/2}$, $^6H_{7/2}$, $^6H_{9/2}$ multiplets of ^6H term of Sm^{3+} ion vary from 93 cm^{-1} to 326 cm^{-1}. Excitation spectrum of sample of nominal composition of $LaIn_{0.98}Sb_{0.02}O_3$ consists of only one band of high intensity with maximum at 324 nm. $LaIn_{0.98}Sb_{0.02}O_3$ sample shows a PL band with maximum at 430 nm referred to Sb^{3+} ion and $La_{0.98}Sm_{0.02}InO_3$ sample shows excitation band with maximum at 408 nm referred to Sm^{3+} ion. These results demonstrate that for the sample of nominal composition of $La_{0.98}Sm_{0.02}In_{0.98}Sb_{0.02}O_3$ the condition of effective absorbed energy transfer from sensitizer (Sb^{3+}) to activator (Sm^{3+}) which is required for sensitizing effect of Sb^{3+} on Sm^{3+} is met. It was established that PL bands intensity of spectra obtained after $\lambda_{ex}=320$, 405 and 470 nm for $La_{0.98}Sm_{0.02}In_{0.98}Sb_{0.02}O_3$ sample with small amount ($\approx 5\%$) of $La_{1-y}Sm_ySbO_3$ impurity is much higher than that of single-phased $La_{0.98}Sm_{0.02}InO_3$ solid solution. Such a significant $La_{0.98}Sm_{0.02}In_{0.98}Sb_{0.02}O_3$ PL intensity increase could be caused by sensitizing effect of Sb^{3+} on Sm^{3+} photoluminescence. Although it can't be excluded that the reason could be higher PL of Sm^{3+} and Sb^{3+} ions in impurity $La_{1-y}Sm_ySbO_3$ matrix than in main phase $LaInO_3$-based matrix. In accordance to that it is possible that PL intensity of samples containing both Sm^{3+} and Sb^{3+} ions is mainly due to impurity phase PL, but not that of main phase.

Acknowledgments

Financial support of bilateral Belarus-Latvia program is greatly acknowledged.

References

[1] X. Liu, J. Lin, Solid State Sci. 11 (2009) 2030.
[2] N. Laksminarasimhan, U.V. Varadaraju, Mater. Res. Bull. 41 (2006) 724.
[3] An Tang, D. Zhang, L. Yang, X. Wang, Optoelectron. Adv. Mater. 5 (10) (2011) 1031.
[4] L.I. van Steensel, S.G. Bokhove, A.M. van de Craats, J. de Blank, G. Blasse, Mater. Res. Bull. 30 (11) (1995) 1359.
[5] E.W.J.L. Oomen, L.C.G. van Gorkom, W.M.A. Smit, G. Blasse, J. Solid State Chem. 65 (1986) 156.
[6] L. Chen, G. Yang, J. Liu, X. Shu, G. Zhang, Y. Jiang, J. Appl. Phys. 105 (2009) 013513.
[7] L. Chen, Y. Jiang, S. Chen, G. Zhang, C. Wang, G. Li, J. Lumin. 128 (2008) 2048.
[8] L. Chen, X. Deng, S. Xue, A. Bahader, E. Zhao, Y. Mu, H. Tian, S. Lü, K. Yu, Y. Jiang, S. Chen, Y. Tao, W. Zhang, J. Lumin. 149 (2014) 144.
[9] L. Chen, A. Luo, X. Deng, S. Xue, Y. Zhang, F. Liu, J. Zhu, Z. Yao, Y. Jiang, S. Chen, J. Lumin. 143 (2013) 670.
[10] L. Chen, A.Q. Luo, Y. Zhang, X.H. Chen, H. Liu, Y. Jiang, S.F. Chen, K.J. Chen, H. C. Kuo, Y. Tao, G.B. Zhang, J. Solid State Chem. 201 (2013) 229.
[11] M.P. Shaskolskaya, Crystallography, in: Handbook for Universities, Vysshaya shkola: Moscow, Russia, 1976, 391 p.
[12] S. Krupicka, The Physics of Ferrites and Related Magnetic Oxides, Mir: Moscow, Russia, 1976, 325 p.
[13] JCPDS 03-065-2426.
[14] JCPDS 00-034-1130.
[15] J. Kaur, D. Singh, N.S. Suryanarayana, V. Dubey, J. Disp. Technol. 99 (2016) 1.
[16] X. Liu, J. Lin, J. Mater. Chem. 18 (2007) 221.
[17] I.N. Kandidatova, Physicochemical Properties of Solid Solutions of Gallates, Indates of Rare-Earth Elements with Perovskite Structure (Ph.D. Thesis), Minsk, Sept. 2014.
[18] R. Karlin, Magneto-Chemistry, Mir: Moscow, Russia, 1989, 400 p.
[19] G. Blasse, Mater. Chem. Phys. 16 (1987) 201.